Contribution from the Department of Chemistry,
University of Leuven, Celestijnenlaan 200F, 3001 Heverlee-Leuven, Belgium

Photochemistry of Chromium(III) Ammine Compounds: An ab Initio Study

L. G. Vanquickenborne,* B. Coussens, D. Postelmans, A. Ceulemans,* and K. Pierloot

Received January 3, 1991

In this work, we report the first ab initio study of the photochemistry of some chromium(III) ammine complexes: $Cr(NH_3)_5F^{2+}$, *trans*-$Cr(NH_3)_4X_2^+$ (X = F^-, Cl^-), and *cis*-$Cr(NH_3)_4F_2^+$. A dissociative mechanism is adopted and the photoinduced substitution reactions are considered to be the result of three separate processes: (1) the selective loss of a ligand from the complex in its first excited state, (2) the isomerization of the so-formed pentacoordinated fragment, and (3) the association of this fragment with an entering solvent ligand. For all complexes, the ab initio method leads to a correct identification of the photoactive state. Moreover, the electron density shifts upon excitation can be correlated rather nicely with the preferential leaving ligand as observed experimentally. For $Cr(NH_3)_5F^{2+}$ and trans-$Cr(NH_3)_4Cl_2^+$ the isomerization pathways of the relevant pentacoordinated fragments are studied by using Woodward-Hoffmann state correlation diagrams. These diagrams are further combined into a single reaction surface of a Jahn-Teller type. The stereomobility of the Cr(III) photochemical substitution reactions is rationalized in terms of a single rule which describes the deactivation pathways on this surface. The ab initio results are in remarkable agreement with the earlier ligand field calculations.

I. Introduction

The photochemical substitution reactions of chromium(III) ammine compounds form one of the traditional topics of inorganic photochemistry. Even today, the experimental data on this topic are accumulating increasingly fast. As it appears however, many important questions remain still open. For instance, is there a well-defined excited state from which the ligand photochemistry occurs, and if so, what is the electronic configuration and the equilibrium geometry of the molecule in that state? Also, there is a continuing controversy on the specific mechanism of the ligand substitution reactions.[1-10]

However, two features of the chromium(III) ammine photochemistry are very well established. One of these is the oriented labilization, the other shows up in the stereochemical aspects of the substitution reactions. Already in the early 1970s, the available experimental data led Kirk to the formulation of the following stereochemical rule: "The entering ligand will stereospecifically occupy a position corresponding to entry into the coordination sphere trans to the leaving ligand."[2] This rule suggests that the photochemical substitution reactions are essentially stereomobile. A second important contribution has been the proposal by Adamson of two empirical rules that would predict the site specificity of the photolabilization: (1) the leaving ligand is situated on the axis having the weakest ligand field; (2) of the two ligands situated on the labilized axis, the leaving ligand is the one exhibiting the strongest ligand field.[11] The first of these rules is remarkably well obeyed, not only for Cr(III) complexes but also for strong field d^6 complexes. The second rule though seems to lack a theoretical basis,[7] and is indeed much less general.

The photochemistry of chromium(III) amine compounds also attracted attention from the theoretical point of view. Several research groups have attempted to find a general theoretical basis for the leaving ligand "rules" and the apparent exceptions.[12-21] Moreover, Vanquickenborne and Ceulemans presented a rationalization of the stereomobility of the Cr(III) photochemical substitution reactions.[22] Yet, all of these theoretical approaches are based on semiempirical methods, mainly ligand field models.

It is the purpose of the present paper to investigate the Cr(III) photochemistry by means of more rigorous ab initio calculations. The following compounds were selected: $Cr(NH_3)_5F^{2+}$, the two isomers (trans and cis) of $Cr(NH_3)_4F_2^+$ and the *trans*-$Cr(NH_3)_4Cl_2^+$ complex. A previous paper presents a detailed analysis of the ground states and of the ligand field spectra[23] of these complexes. Here, for each complex, the preferential labilization is discussed, and for $Cr(NH_3)_5F^{2+}$ and the dichloro compound, the stereomobility of the photochemical substitution reaction is also analyzed in some detail.

II. Experimental Data

a. Nature of the Leaving Ligand and Photostereochemistry. *trans*-$Cr(NH_3)_4Cl_2^+$ is one of the typical *trans*-diacidotetrammine complexes where the leaving ligand is determined by Adamson's first rule.[24] Irradiation in the lowest excited quartet band leads almost exclusively (>90%) to Cl^- aquation. Moreover, the resulting reaction product mainly possesses a cis configuration

$$\textit{trans}\text{-}Cr(NH_3)_4Cl_2^+ + H_2O \xrightarrow{h\nu} \textit{cis}\text{-}Cr(NH_3)_4(H_2O)Cl^{2+} + Cl^-$$

For the related reaction

$$Cr(NH_3)_5Cl^{2+} + H_2O \xrightarrow{h\nu} \textit{cis}\text{-}Cr(NH_3)_4(H_2O)Cl^{2+} + NH_3$$

it has been established unequivocally that the NH_3 ligand was released from the heteroaxis,[25] satisfying both Kirk's and Adamson's rules. Therefore it came as a surprise when it was discovered that the photoaquation of $Cr(NH_3)_5F^{2+}$ appeared to be less simple.[26,27] Although the preferred reaction mode was still ammonia loss, both cis and trans isomers of $Cr(NH_3)_4(H_2O)F^{2+}$ were being formed in a 85:15 ratio. Furthermore a study of the analogous *trans*-$Cr(en)_2(NH_3)F^{2+}$ complex clearly showed that the axial ammonia could only account for 78% of the total ammine loss, the remaining 22% being due to labilization of the equatorial

(1) Sýkora, J.; Šima, J. *Coord. Chem. Rev.* **1990**, *107*.
(2) Kirk, A. D. *Mol. Photochem.* **1973**, *5*, 127.
(3) Adamson, A. W.; Fleischauer, P. D. *Concepts of Inorganic Photochemistry*; Wiley: New York, 1975.
(4) Wrighton, M. S. *Top. Curr. Chem.* **1976**, *65*, 37.
(5) Adamson, A. W. *Pure Appl. Chem.* **1979**, *51*, 313.
(6) Kirk, A. D. *Coord. Chem. Rev.* **1981**, *39*, 225.
(7) Vanquickenborne, L. G.; Ceulemans, A. *Coord. Chem. Rev.* **1983**, *48*, 157.
(8) Larkworthy, L. F. *Coord. Chem. Rev.* **1984**, *57*, 189.
(9) Endicott, J. F.; Ramasami, T.; Tamilarasan, R.; Lessard, R. B.; Ryu, C. K.; Brubaker, G. R. *Coord. Chem. Rev.* **1987**, *77*, 1.
(10) Mønsted, L.; Mønsted, O. *Coord. Chem. Rev.* **1989**, *94*, 109.
(11) Adamson, A. W. *J. Phys. Chem.* **1967**, *71*, 798.
(12) Zink, J. I. *Mol. Photochem.* **1973**, *5*, 151.
(13) Zink, J. I. *J. Am. Chem. Soc.* **1972**, *94*, 8039.
(14) Zink, J. I. *Inorg. Chem.* **1973**, *12*, 1957.
(15) Zink, J. I. *J. Am. Chem. Soc.* **1974**, *96*, 4464.
(16) Wrighton, M.; Gray, H. B.; Hammond, G. S. *Mol. Photochem.* **1973**, *5*, 165.
(17) Furlani, C. *Theor. Chim. Acta* **1974**, *34*, 233.
(18) Vanquickenborne, L. G.; Ceulemans, A. *J. Am. Chem. Soc.* **1977**, *99*, 2208.
(19) Vanquickenborne, L. G.; Ceulemans, A. *Inorg. Chem.* **1979**, *18*, 3475.
(20) Kirk, A. D. *Inorg. Chem.* **1979**, *18*, 2326.
(21) Vanquickenborne, L. G.; Ceulemans, A. *Inorg. Chem.* **1979**, *18*, 897.
(22) Vanquickenborne, L. G.; Ceulemans, A. *J. Am. Chem. Soc.* **1978**, *100*, 475.
(23) Vanquickenborne, L. G.; Coussens, B.; Postelmans, D.; Ceulemans, A.; Pierloot, K. *Inorg. Chem.* **1991**, *30*, 2978.
(24) Riccieri, P.; Zinato, E. *J. Am. Chem. Soc.* **1975**, *97*, 6071.
(25) Zinato, E.; Riccieri, P.; Adamson, A. W. *J. Am. Chem. Soc.* **1974**, *96*, 375.
(26) Wright, R. E.; Adamson, A. W. *Inorg. Chem.* **1977**, *16*, 3360.
(27) Wong, C. F. C.; Kirk, A. D. *Inorg. Chem.* **1977**, *16*, 3148.

0020-1669/92/1331-0539$03.00/0

ligands.[27] If one assumes that photosubstitution of the axial ammine is 100% stereomobile and that the ratio of quantum yields Φ_{ax}/Φ_{eq} in $Cr(NH_3)_5F^{2+}$ is comparable to the ratio Φ_{NH_3}/Φ_{en} in *trans*-$Cr(en)_2(NH_3)F^{2+}$, one has for irradiation with 546 nm light at 10 °C:

$$Cr(NH_3)_5F^{2+} \xrightarrow{78\%} cis\text{-}Cr(NH_3)_4F(H_2O)^{2+} + (NH_3)_{ax}$$

$$\xrightarrow{22\%} \begin{cases} 30\%\ cis\text{-}Cr(NH_3)_4F(H_2O)^{2+} \\ 70\%\ trans\text{-}Cr(NH_3)_4F(H_2O)^{2+} \end{cases} + (NH_3)_{eq}$$

The second assumption may be incorrect in detail, since ethylenediamine loss is probably slightly favored over NH_3 loss due to steric strain.[28] In any case it is clear that axial ammine loss is not the only reaction mode. Furthermore axial and equatorial modes seem to be characterized by complementary stereochemistries.

Kirk and Frederick also investigated the photochemistry of the *trans*- and *cis*-$Cr(NH_3)_4F_2^+$ isomers.[29] For both compounds, they observed efficient ammonia aquation with only minor yields of fluoride. Moreover, an analysis of the reaction products revealed that these consisted almost exclusively of only two isomers, namely 1,6-difluoro-2-aquotriamminechromium(III) (*mer*-FWF) and 1,2-difluoro-6-aquotriamminechromium(III) (*mer*-WFF):

$$trans\text{-}Cr(NH_3)_4F_2^+ \xrightarrow{h\nu} 30\%\ mer\text{-FWF} + 70\%\ mer\text{-WFF}$$

$$cis\text{-}Cr(NH_3)_4F_2^+ \xrightarrow{h\nu} 45\%\ mer\text{-FWF} + 55\%\ mer\text{-WFF}$$

Formation of the 1,2-difluoro-3-aquotriamminechromium(III) (*fac*-WFF) was barely discernible. Note that the ammine photolysis in the trans product is an exception to Adamson's rules, which predict predominant release of the F^- ions. Furthermore the absence of the *fac*-WFF product in a photolyzed solution of *cis*-$Cr(NH_3)_4F_2^+$ is in contradiction with Kirk's rule, which predicts predominance of the facial isomer.[6]

b. Photoreactive Excited State and Mechanism of the Photosubstitution Reaction. In the conventional view of Cr(III) photosubstitutions, the photoreactions originate from a thermally equilibrated excited quartet state, with a distorted geometry.[3] The decay of this so-called "thexi" state is essentially determined by a Boltzmann distribution over the available decay channels. This scheme is indicated with the acronym DERCOS, for decay via random coordinate selection. In 1981 Langford et al. introduced the contrasting new idea that the photoprocess might exhibit nonequilibrium dynamics.[30] In this view the photoprocess is thought to occur at a very fast time scale which is comparable to vibrational relaxation times. This behavior was called DOSENCO behavior (decay on a specific nuclear coordinate) to emphasize the preferential selection of a specific reaction channel. Some scattered experimental results, involving ultrafast laser experiments[31] and wavelength dependence studies,[9] were interpreted along these lines. In addition theoretical selection rules for the DOSENCO coordinate were derived. In the case of the $^4A_{2g}$–$^4T_{2g}$ excitation of Cr(III) complexes, the specific reactive coordinate was identified as a highly excited t_{1u} buckle mode.[32] According to Langford et al., decay along this mode would give rise to associative ligand replacement.[30]

It should be pointed out that the selection rules on which this analysis was based are not confirmed by detailed spectral studies.[33,34] It is indeed well established that the quartet transitions in centrosymmetric Cr(III) complexes are forced dipole transitions, involving only *single* quanta excitations of the ungerade allowing modes, such as the t_{1u} buckle mode. Franck–Condon excitations of several vibrational quanta are strictly confined to the Raman modes a_{1g}, e_g, and t_{2g}. The selection rules governing the forced dipole mechanism are well understood in the framework of dynamic ligand field theory.[35] Moreover the distorted structure of the $^4T_{2g}$ excited state, which is at the basis of the observed FC progressions, complies very well with a simple Herzberg–Teller description of a conventional T_{2g} ($a_{1g} + e_g$) Jahn–Teller system.[36] Hence from spectral observations, one predicts that the preferential decay modes of the quartet excited state will involve the JT coordinates, thus giving rise to population of the minima on the JT surface. These minima are characterized by labilized planes of excitation, exactly as considered in the ligand field model,[7] which forms the basis for the present ab initio treatment.

A further point of continuing debate involves the nature of the intimate reaction mechanism. Measurements of activation volumes for the photoreaction point to positive ΔV^* values for cationic complexes and negative values for negatively charged complexes.[37,38] From this it was concluded that the photolysis mechanism in positively charged complexes is of the associative interchange type. This complied with Kirk's earlier proposal of an edge displacement mechanism to account for the extreme stereospecificity of the photoreaction.[2] Since then it has been pointed out on several occasions that seven-coordinated transition states with a pentagonal bipyramidal or octahedral wedge geometry will not give rise to the desired stereospecificity.[1,7,9] A subsequent suggestion by Endicott[39] that a face-capped trigonal prism might intervene seems even more unlikely since such a transition state implies a scrambling of all ligands and therefore a total loss of stereochemical information. Furthermore, the existing theoretical studies clearly indicate that Adamson's rules can only be explained if the mechanism of the photoreaction is initiated by a bond-breaking step. From this it may be concluded that, although specific solvent interactions are important, associative mechanisms cannot account for the observations. Studies of the roles of the entering anion and of steric hindrance in the photolysis of amminechromium(III) complexes seem to support this conclusion.[40,41]

In our opinion a major breakthrough in this debate can only be reached by studying possible reaction intermediates in inert matrices at very low temperature.

III. Details of the ab Initio Calculations

As in the previously given ligand field rationalization,[22] we will assume a dissociative mechanism, and the photochemical substitution reactions are formally dissected in three separate processes: (1) selective ligand loss from the complex in its first excited state, (2) the isomerization of the so-formed pentacoordinated intermediate, and (3) the association of this intermediate with an entering solvent ligand. Processes (2) and (3) will only be discussed for $Cr(NH_3)_5F^{2+}$ and the *trans*-$Cr(NH_3)_4Cl_2^+$ complex. The pentacoordinated intermediates that must be considered for these compounds are the square pyramids (SP) and trigonal bipyramids (TBP) of the $Cr(NH_3)_4X^{2+}$ (X = F^- or X = Cl^-) fragments. In the SP structures, the X ligand can be in apical (SP_{ap}) or in basal (SP_{bas}) position; in the TBP intermediates, the X ligand may occupy an axial (TBP_{ax}) or an equatorial (TBP_{eq}) site.

For the intermediates as well as for the hexacoordinated starting compounds, we made use of a formalism, detailed in refs 42 and 43. The energies of the individual states were obtained by carrying

(28) Kirk, A. D. *Inorg. Chem.* **1979**, *18*, 2326.
(29) Kirk, A. D.; Frederick, L. A. *Inorg. Chem.* **1981**, *20*, 60.
(30) Hollebone, B. R.; Langford, C. H.; Serpone, N. *Coord. Chem. Rev.* **1981**, *39*, 181.
(31) Rojas, G. E.; Dupuy, C.; Sexton, D. A.; Magde, D. *J. Phys. Chem.* **1986**, *90*, 87.
(32) Hollebone, B. R. *Theor. Chim. Acta* **1980**, *56*, 45.
(33) Wilson, R. B.; Solomon, E. I. *Inorg. Chem.* **1978**, *17*, 1729.
(34) Güdel, H. U.; Snellgrove, T. R. *Inorg. Chem.* **1978**, *17*, 1617.
(35) Ceulemans, A.; Bongaerts, N. *Theor. Chim. Acta* **1990**, *77*, 85.
(36) Schmidtke, H.-H.; Degen, J. *Struct. Bonding* **1989**, *71*, 99.
(37) Angermann, K.; Vom Eldik, R.; Kelm, H.; Wasgestian, F. *Inorg. Chem.* **1981**, *20*, 955.
(38) Angermann, K.; Vom Eldik, R.; Kelm, H.; Wasgestian, F. *Inorg. Chim. Acta* **1981**, *49*, 247.
(39) Endicott, J. F. *Comments Inorg. Chem.* **1985**, *3*, 349.
(40) Krause, H. H.; Wasgestian, F. *Inorg. Chim. Acta* **1981**, *49*, 231.
(41) Wasgestian, F.; Gourin, E. *Inorg. Chim. Acta* **1986**, *120*, L17.
(42) Vanquickenborne, L. G.; Haspeslagh, L.; Hendrickx, M.; Verhulst, J. *Inorg. Chem.* **1984**, *23*, 1677.
(43) Vanquickenborne, L. G.; Hendrickx, M.; Postelmans, D.; Hyla-Krypsin, I.; Pierloot, K. *Inorg. Chem.* **1988**, *27*, 900.

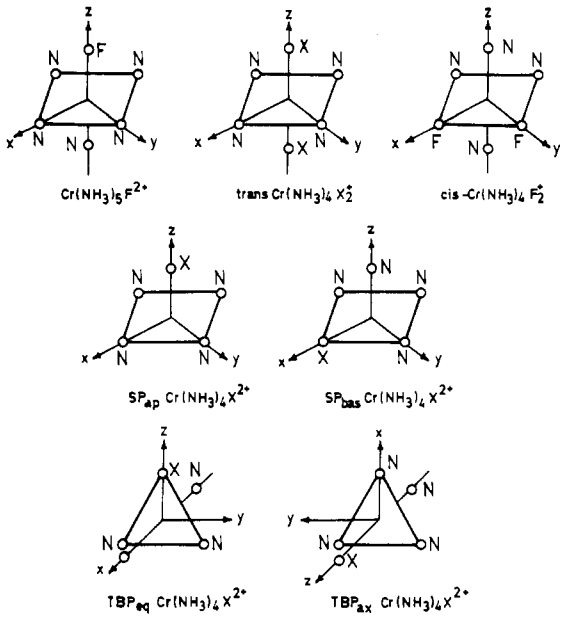

Figure 1. Coordinate systems used in the calculations. X represents the F^- or Cl^- ion; N stands for the NH_3 ligand.

out complete ligand field CI calculations within the d^3 manifold, using the Av(d^3) orbitals, i.e. the Hartree–Fock orbitals of the weighted average of all ligand field states. For this purpose, the FRORB program was used,[44] whereas the Av(d^3) orbitals were obtained by means of the SYMOL program,[45] a computer package that is based on Roothaan's restricted Hartree–Fock formalism for open-shell systems.[46]

All complexes were described by the same basis sets as in our previous work.[23] For the Cr metal ion, we used the rather large (15s,11p,6d/11s,8p,4d) basis set,[47] for the F and N atoms, we used the (9s,5p/5s,3p) bases proposed by Huzinaga and Dunning,[48] for the hydrogen atom, we adopted a (4s/3s) set, and the Cl atom was described by the nonsegmented basis that was introduced by Veillard and Dunning.[49] This combination of basis sets should guarantee near Hartree–Fock limit results and should provide a balanced description of the metal ion and the ligands.[50]

All compounds were assumed to possess idealized geometries; i.e., each ligand–metal–ligand bond axis was taken to be 90 or 120°, and we used only one set of bond lengths. For the Cr–N distance, we chose the average Cr–N length for a number of $Cr(NH_3)_6^{3+}$ ions in different crystal environments, i.e. 2.07 Å.[51-56] The Cr–F distance was set equal to 1.891 Å, i.e. the average Cr–F bond lengths of the two $Cr(NH_3)_4F_2^+$ isomers,[57] and the Cr–Cl distance to 2.33 Å, i.e. the experimental value for the *trans*-$Cr(NH_3)_4Cl_2^+$ complex.[58] The geometrical parameters for the NH_3 ligand were taken to be identical with those for the free NH_3 molecule in the gas phase: R(N–H) = 1.02 Å and θ(H–N–H) = 106.6°.[59] In each compound, the Cr–NH_3 units were assumed to have C_{3v} symmetry and the hydrogen atoms were arranged in such a manner that $Cr(NH_3)_5F^{2+}$ and the SP_{bas} structures could be calculated in C_s symmetry, the two trans complexes and the SP_{ap} intermediates in C_{4v} symmetry, the TBP_{ax} structures in C_{3v}, and the other compounds in C_{2v} symmetry. For $Cr(NH_3)_5F^{2+}$, the C_{4v} and the C_{3v} complexes as well as the TBP_{eq} intermediates, the heteroligands were placed on the z axis; for the cis compound, one F^- ion was placed on the x axis with the other one on the y axis, and for the SP_{bas} fragments the heteroligand was placed on the x axis. (See Figure 1.)

Table I. Excitation Energies (cm^{-1}) from the $^4B_1$ Ground State to the Lowest Excited Quartet States[a] for the Four Complexes under Consideration[b]

	$^4B_1 \rightarrow {}^4B_2$		$^4B_1 \rightarrow {}^4E$	
complex	LFT	ab initio	LFT	ab initio
$Cr(NH_3)_5F^{2+}$	21 540	18 877	19 992	17 953[c]
trans-$Cr(NH_3)_4F_2^+$	21 540	18 134	18 434	16 561
trans-$Cr(NH_3)_4Cl_2^+$	21 540	18 716	17 102	15 742
cis-$Cr(NH_3)_4F_2^+$[a]	18 455	16 901	19 993	17 254[c]

[a] The energy levels are classified in the holohedron D_{4h} symmetry, rather than in the actual C_{2v} symmetry. Labels are given without the gerade parity subscript. [b] The ligand field and ab initio values are the result of a CI calculation considering all states originating from the d^3 configuration. Within LFT, this CI calculation was carried out with the semiempirical parameters of ref 7; the ab initio CI calculation was performed within a frozen orbital approach, using the Av(d^3) orbitals. [c] Within the actual symmetry, which is C_s for $Cr(NH_3)_5F^{2+}$ and C_{2v} for the cis compound, the ab initio energies for the two ^4E components are slightly different. The values given in this table refer to the average of these two numbers.

Table II. Composition of the Photoactive State for the Four Complexes under Consideration[a]

	photoactive	LFT		ab initio	
complex	state	% d_{z^2}	% $d_{x^2-y^2}$	% d_{z^2}	% $d_{x^2-y^2}$
$Cr(NH_3)_5F^{2+}$	^4E	73.0	27.0	70.0	30.0
trans-$Cr(NH_3)_4F_2^+$	^4E	70.9	29.1	62.5	37.5
trans-$Cr(NH_3)_4Cl_2^+$	^4E	87.5	12.5	81.8	18.2
cis-$Cr(NH_3)_4F_2^+$	$^4B_2$	0.0	100.0	0.0	100.0

[a] For $Cr(NH_3)_5F^{2+}$ and the two trans complexes, this table gives the contribution of the $(d_{xz},d_{yz}) \rightarrow d_{z^2}$ and the $(d_{xz},d_{yz}) \rightarrow d_{x^2-y^2}$ excitation to the lowest excited ^4E. For the cis compound, % d_{z^2} and % $d_{x^2-y^2}$ respectively refer to the contribution of the $d_{xy} \rightarrow d_{x^2-y^2}$ and the $d_{xy} \rightarrow d_{z^2}$ excitation to the lowest excited $^4B_2$ state.

IV. The Leaving Ligand Problem

A study of the leaving ligand problem requires the identification of the photoreactive state. The picture emerging from the literature is that the photoreaction occurs in two distinct stages. A relatively minor fraction is formed at a very short time scale (subnanosecond), while the remaining fraction is formed at the time scale of doublet emission (microsecond). In the case of *trans*-$Cr(en)_2F_2^+$, which is analogous to the *trans*-difluoro complex treated here, only the slow component could be observed.[60] There seems to be a general consensus that the ultrafast fraction is due to direct reaction of the lower quartet state, while the slow fraction reflects a delayed quartet reactivity. In this picture the doublet merely acts as a reservoir from which the reactive quartet is populated. Waltz et al.[60] have suggested that this may be different for the *trans*-difluoro compound, which is known to have different emission properties. Nonetheless it should be remarked that the emission lifetime of this complex correlates very well with the estimated activation barrier for back-intersystem crossing to the quartet state.[9,61] Hence the subsequent analysis will primarily

(44) FRORB was written by K. Pierloot, Laboratory of Quantum Chemistry, University of Leuven.
(45) Van der Velde, G. A. Ph.D. Thesis, Rijksuniversiteit Groningen, 1974.
(46) Roothaan, C. C. J. *Rev. Mod. Phys.* **1951**, *23*, 69; **1960**, *32*, 179.
(47) Vanquickenborne, L. G.; Verhulst, J. *J. Am. Chem. Soc.* **1983**, *105*, 1769.
(48) Dunning, T. H. *J. Chem. Phys.* **1970**, *53*, 2823. Huzinaga, S. *J. Chem. Phys.* **1965**, *42*, 1293.
(49) Veillard, A. *Theor. Chim. Acta* **1968**, *12*, 405. Dunning, T. H. *Chem. Phys. Lett.* **1970**, *7*, 423.
(50) Vanquickenborne, L. G.; Verhulst, J.; Coussens, B.; Hendrickx, M.; Pierloot, K. *THEOCHEM* **1987**, *153*, 227.
(51) Raymond, K. N.; Meek, D. W.; Ibers, J. A. *Inorg. Chem.* **1968**, *7*, 1111.
(52) Goldfield, S. A.; Raymond, K. N. *Inorg. Chem.* **1971**, *10*, 2604.
(53) Wieghardt, Von K.; Weiss, J. *Acta Crystallogr.* **1972**, *B28*, 529.
(54) Clegg, W.; Greenhalgh, D. A.; Straughan, B. P. *J. Chem. Soc., Dalton Trans.* **1975**, 2591.
(55) Clegg, W. *Acta Crystallogr.* **1976**, *B32*, 2907.
(56) Clegg, W. *J. Chem. Soc. Dalton Trans.* **1982**, 593.
(57) Brenčič, J. V.; Čeh, B.; Leban, I. *Monatsh. Chem.* **1981**, *112*, 1359.
(58) Brenčič, J. V.; Leban, I.; Zull, J. *Z. Anorg. Allg. Chem.* **1985**, *521*, 199.
(59) Hamilton, W. C.; Ibers, J. A. *Hydrogen Bonding in Solids*; W. C. Benjamin Inc.: New York, 1968.
(60) Waltz, W. L.; Lilie, J.; Lee, S. H. *Inorg. Chem.* **1984**, *23*, 1768.
(61) Linck, N. J.; Berens, S. J.; Magde, D.; Linck, R. G. *J. Phys. Chem.* **1983**, *87*, 1733.

focus on the electronic characteristics of the lowest excited quartet states.

a. Composition and energies of the Lowest Excited Quartet States. The excitation energies to the relevant quartet states are tabulated in Table I. As well-known, the semiempirical ligand field results[7] are quite close to the experimental values. Although the ab initio values are systematically smaller, the ab initio method predicts the same relative ordering of the $^4B_2$ and ^4E components as the ligand field model. For $Cr(NH_3)_5F^{2+}$ and the two trans complexes, the predominant photoactive level is identified as the ^4E state; for the cis compound, it turns out to be the $^4B_2$ component. These facts can readily be rationalized from first-order ligand field theory

$$E(^4B_2) - E(^4E;^4T_{2g}) = \tfrac{1}{2}(10\overline{Dq}_{eq} - 10\overline{Dq}_{ax})$$

where $10\overline{Dq}_{ax}$ represents the average spectrochemical strength of the ligands on the z axis and $10\overline{Dq}_{eq}$ stands for the average spectrochemical strength of the ligands on the x or y axis. Therefore, when $10\overline{Dq}_{eq} > 10\overline{Dq}_{ax}$, the ^4E state is the photoactive level, but when $10\overline{Dq}_{eq} < 10\overline{Dq}_{ax}$, the $^4B_2$ component becomes the photoactive state. As the ab initio $^4T_{2g}$ splittings have the same sign as the ligand field splittings, the ab initio method supports the ligand field idea that the F^- and Cl^- ion are weaker field ligands than the NH_3 molecule.[62]

In Table II, the composition of the photoactive states is given. As can be seen, the $^4B_2$ component refers to a $d_{xy} \rightarrow d_{x^2-y^2}$ excitation while the ^4E states correspond predominantly to a $(d_{xz},d_{yz}) \rightarrow d_{z^2}$ transition with a smaller contribution of the $(d_{xz},d_{yz}) \rightarrow d_{x^2-y^2}$ excitation. If the complexes were perfectly octahedral, the d_{z^2} content would be precisely 75%. According to ligand field theory the fraction of d_{z^2} in the $^4E(^4T_{2g})$ state, x, is given by[14,18]

$$x = (1 + c^2)^{-2}\left[\frac{\sqrt{3} - c}{2}\right]^2$$

where c is defined as

$$c = \frac{\sqrt{3}(\bar{\sigma}_{ax} - \bar{\sigma}_{eq})}{24B}$$

In a perfect octahedron, $x = {}^3/_4$, and its value decreases if $\bar{\sigma}_{ax} > \bar{\sigma}_{eq}$. Since the F^- ion is considered to be a stronger σ donor than the NH_3 molecule, it will lower the d_{z^2} content when coordinated axially. Obviously this effect will be more pronounced in the *trans*-difluoro compound than in the monofluoro complex, because of the larger c value. The Cl^- ligand is expected to induce the opposite trend, being a weaker σ donor than NH_3. As Table II indicates, the ab initio results are in qualitative agreement with this ligand field analysis. From this point of view, the ab initio calculations do confirm the relative σ-donor strengths in the series $F^- > NH_3 > Cl^-$.

From a quantitative point of view, the contribution of the $(d_{xz},d_{yz}) \rightarrow d_{x^2-y^2}$ excitation appears to be more important at the ab initio level than in ligand field theory.

b. Prediction of the Leaving Ligand. The development of theoretical models to predict the specific labilization site has been stimulated by the empirical rules of Adamson,[5] which were later modified by the I^* model.[18] This model is now widely being used in photolability studies.[9,63] It applies the angular overlap approximation to calculate orbital populations and to generate a set of parameters I^*(M–L) which are considered to be roughly proportional to the metal–ligand bond strengths in the photoactive state. These parameters are defined as

$$I^*(M\text{–}L) = \sum_i h_i \langle d_i|V_L|d_i\rangle$$

where the summation runs over the five d orbitals, h_i is the number of holes in the ith d orbital and $\langle d_i|V_L|d_i\rangle$ is the destabilization energy of that orbital under the ligand field potential V_L, i.e. the potential of the individual ligand L. The "leaving ligand" is considered to be the ligand with the lowest value of I^*(M–L).

An analogous set of bond indices, I(M–L), can be generated for the ground state of a given complex and it has been shown that the labilization energies $I - I^*$ are directly related to Adamson's rules. As a matter of fact, these rules can be restated as: "The leaving ligand is the one characterized by the largest $I - I^*$ value". When Adamson's rules are valid, the $I - I^*$ model leads to the same conclusions as the I^* parameters but when they are not, the I^* indices apparently have a better predictive value. This is illustrated in Table III, listing both the $I - I^*$ and the I^* values for the four complexes under consideration. Later on, we will compare these parameters with our ab initio results, and therefore, Table III gives—besides total values—also σ and π constituent parts. For $Cr(NH_3)_5F^{2+}$, the cis compound, and the *trans*-dichloro complex, the specific labilization site is determined by Adamson's rules and the $I - I^*$ model predicts the same reaction mode as the I^* parameters. However, for *trans*-$Cr(NH_3)_4F_2^+$, Adamson's rules and the $I - I^*$ indices predict preferential F^- aquation and only the I^* model is compatible with the observed NH_3 release.

At the ab initio level considered in the present paper, no quantitative bond energies can be expected. Indeed, electron correlation as well as solvation effects are neglected (the calculations are carried out for the isolated complexes). It must also be kept in mind that the calculations are based on ground-state geometries. No optimization of the excited state geometry was attempted. In contrast attention is focused on the primary labilization of the different ligands due to sudden changes in the electron density that are caused by the vertical excitation process. These changes can explicitly be evaluated by making use of the Mulliken population analysis, i.e. by subtracting the Mulliken gross populations in the photoactive state (p^*) from those in the ground state (p). It turns out that the "leaving ligand" always corresponds to the ligand that exhibits the largest decrease of total donation to the central metal ion $\Delta p = p^* - p$. Table III also shows the results of such a Mulliken population analysis.

Positive values of Δp correspond to a larger population of the relevant ligand orbitals in the excited state, implying a weaker ligand to metal donation. A direct comparison between ligand populations and bond indices seems rather irrelevant, since they refer to completely different physical quantities: the bond indices, intended to be a measure for the bond strength, depend on both ionic and covalent contributions, whereas the Mulliken population analysis offers an overall picture of the charge distribution. However, a comparison between Δp and the $I - I^*$ values of Table III reveals a very striking parallellism. Indeed, consider for instance the $^4B_1 \rightarrow {}^4E$ transition for the $Cr(NH_3)_5F^{2+}$ complex. As the ligand field model assumes that $\pi_{NH_3} = 0$, the $I - I^*(\pi)$ values for the Cr–NH_3 bonds are calculated to be zero. So, according to Table III, the Cr–NH_3 π interactions are not affected by the excitation process. The ab initio results substantiate this assumption: they indicate that the NH_3 pπ populations do not change on going from the $^4B_1$ to the ^4E state. For the Cr–F^- bond, the $I - I^*(\pi)$ value appears to be negative. So, the π interaction between Cr and F^- should be strengthened upon excitation. Table III indeed shows that the F^- ion behaves as a better π donor in ^4E than in the ground state. The $I - I^*(\sigma)$ parameters are all positive, suggesting that all metal–ligand σ interactions are weakened as a consequence of the $^4B_1 \rightarrow {}^4E$ transition. Again, the Mulliken population analysis confirms this: in the ^4E state all ligands are seen to be weaker σ donors than in the ground state. Moreover, in accordance with the $I - I^*$ values, the σ donation of the F^- ion is more affected than the σ donation of $(NH_3)_{ax}$ and the σ bond between Cr and $(NH_3)_{ax}$ is weakened to a greater extent than the σ bond between Cr and $(NH_3)_{eq}$.

There is a similar parallelism between Δp and $I - I^*$ for the other complexes as well. Apparently, the bond index differences $I - I^*$ are—to a significant extent—equivalent to the description

(62) The same conclusion was reached in our previous paper[23] where the ab initio excitation energies were fitted to the ligand field CI energy expressions to obtain a "theoretical" set of ligand field parameters.

(63) Herbert, B.; Reinhard, D.; Saliby, M. J.; Sheridan, P. S. *Inorg. Chem.* **1987**, *26*, 4024.

Table III. Values for Each Metal–Ligand Bond of I^*, $I - I^*$ and $\Delta p = p^* - p$ for the Four Complexes under Consideration[a]

		$Cr(NH_3)_5F^{2+}$ (^4E)	*trans*-$Cr(NH_3)_4F_2^+$ (^4E)	*trans*-$Cr(NH_3)_4Cl_2^+$ (^4E)	*cis*-$Cr(NH_3)_4F_2^+$ ($^4B_2$)
$X(\sigma)$	I^*	9.69	9.85	6.26	9.54
	$I - I^*$	5.57	5.41	4.86	5.72
	Δp	0.031	0.023	0.041	0.031
$X(\pi)$	I^*	5.64	5.64	2.70	5.64
	$I - I^*$	−1.88	−1.88	−0.90	−1.88
	Δp	−0.016	−0.012	−0.013	−0.013
$X(\sigma + \pi)$	I^*	15.33	15.49	8.96	15.18
	$I - I^*$	3.69	3.53	3.96	3.84
	Δp	0.015	0.011	0.028	0.018
$N_{ax}(\sigma)$	I^*	9.12			14.36
	$I - I^*$	5.24			0.00
	Δp	0.023			0.000
$N_{ax}(\pi)$	I^*	0.00			0.00
	$I - I^*$	0.00			0.00
	Δp	0.000			0.000
$N_{ax}(\sigma + \pi)$	I^*	9.12			14.36
	$I - I^*$	5.24			0.00
	Δp	0.023			0.000
$N_{eq}(\sigma)$	I^*	11.60	11.52	12.12	8.98
	$I - I^*$	2.76	2.84	2.24	5.38
	Δp	0.017	0.016	0.012	0.021
$N_{eq}(\pi)$	I^*	0.00	0.00	0.00	0.00
	$I - I^*$	0.00	0.00	0.00	0.00
	Δp	0.000	0.000	0.000	0.000
$N_{eq}(\sigma + \pi)$	I^*	11.60	11.52	12.12	8.98
	$I - I^*$	2.76	2.84	2.24	5.38
	Δp	0.017	0.016	0.012	0.021
predicted leaving ligand	I^*	$(NH_3)_{ax}$	$(NH_3)_{eq}$	Cl^-	$(NH_3)_{eq}$
	$I - I^*$	$(NH_3)_{ax}$	F^-	Cl^-	$(NH_3)_{eq}$
	Δp	$(NH_3)_{ax}$	$(NH_3)_{eq}$	Cl^-	$(NH_3)_{eq}$
exptl leaving ligand		$(NH_3)_{ax}$ $(NH_3)_{eq}$	$(NH_3)_{eq}$	Cl^-	$(NH_3)_{eq}$

[a] X stands for F or Cl, N stands for NH_3, the composition of the photoactive states is given in Table II, and I is given in 10^3 cm^{-1}.

of the density shifts upon excitation, as revealed by Δp. It is remarkable that the Δp description should lead to the correct prediction of the leaving ligand in all cases under consideration, even for *trans*-$Cr(NH_3)_4F_2^+$, where the $I - I^*$ model fails. In agreement with ligand field theory, the Δp results in Table III suggest that the σ labilization of the CrF bond is countered by a strengthening of the π bond. At the ab initio level, the total resultant Δp (and the corresponding labilization upon excitation) is larger for NH_3 than for F^-; therefore, in contrast to ligand field theory, the leaving ligand is directly associated with the largest value of Δp. This result is in line with the rationalization of the photochemistry of the related *trans*-$Cr(en)_2F_2^+$ complex that was suggested by Zink.[15]

The Mulliken gross populations of Table III are confirmed by an analysis of the wave functions by means of density difference plots. As an example, Figure 2 shows the electron density shifts upon the $^4B_1 \rightarrow {}^4E$ transition for the $Cr(NH_3)_5F^{2+}$ complex. In the *yz* plane one clearly observes the depopulation of the d_{yz} zone and the population of the d_{z^2} orbital. In the *xy* plane, the contribution of the $(d_{xz}, d_{yz}) \rightarrow d_{x^2-y^2}$ excitation manifests itself by a loss of rotational symmetry of the metal orbitals in that plane. The positive density contours in the $p\sigma$ zones of the ligands are a manifestation of the decreased σ donation. In agreement with Table III, Figure 2 shows the largest build up of charge on the F^- ion and the smallest one for the $(NH_3)_{eq}$ ligands. The strengthening of the Cr–F^- π interactions is evidenced by the negative density contours in the F^- $p\pi$ region, indicating an increased π donation. The fact that no such contours are seen in the $p\pi$ zone of the NH_3 molecules confirms the idea that the π interactions between the chromium ion and the ammonia ligands remain unchanged upon the excitation process. Apparently, unlike the Mulliken population analysis, the qualitative features of Figure 2 do not offer obvious indications on the leaving ligand.

V. Stereomobility of the Photochemical Substitution Reactions

a. Ab Initio Study of the Pentacoordinated Fragments. In a dissociative mechanism the stereochemistry of the photochemical reaction is controlled by the rearrangements of the pentacoordinated fragments that are being formed following ligand dissociation. These pentacoordinated fragments may adopt a square-pyramidal (SP) or trigonal-bipyramidal (TBP) geometry. For the case of the $Cr(NH_3)_4X^{2+}$ fragments, which result from Cl^- loss in *trans*-$Cr(NH_3)_4Cl_2^+$ and NH_3 loss in $Cr(NH_3)_5F^{2+}$, four isomers must be considered: the heteroligand can be in the apical or basal position of the SP or in the axial or equatorial position of the TBP. Interconversions between these isomers can most easily be achieved by bending of a basal axis in the SP:

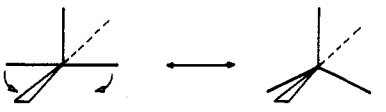

This process is part of the so-called Berry rearrangement, which interchanges sites in pentacoordinated structures. Possible Berry rearrangements of the $Cr(NH_3)_4X^{2+}$ fragment are

$$SP_{ap} \leftrightarrow TBP_{eq} \leftrightarrow SP_{bas} \leftrightarrow TBP_{ax}$$

In all probability the lifetime of these species in solution will be extremely short due to spontaneous binding of solvent molecules. It is noteworthy though that the *trans*-$[Cr(en)_2Br_2]Br \cdot H_2O$ complex and the corresponding chloride containing monohydrate remain photoactive in the solid state, yielding the same *cis*-$Cr(en)_2(H_2O)Br^{2+}$ and *cis*-$Cr(en)_2(H_2O)Cl^{2+}$ products as for the reaction in solution.[64] It may be anticipated that the penta-

(64) Kirk, A. D.; Warren, P. A. *Inorg. Chem.* **1985**, *24*, 720.

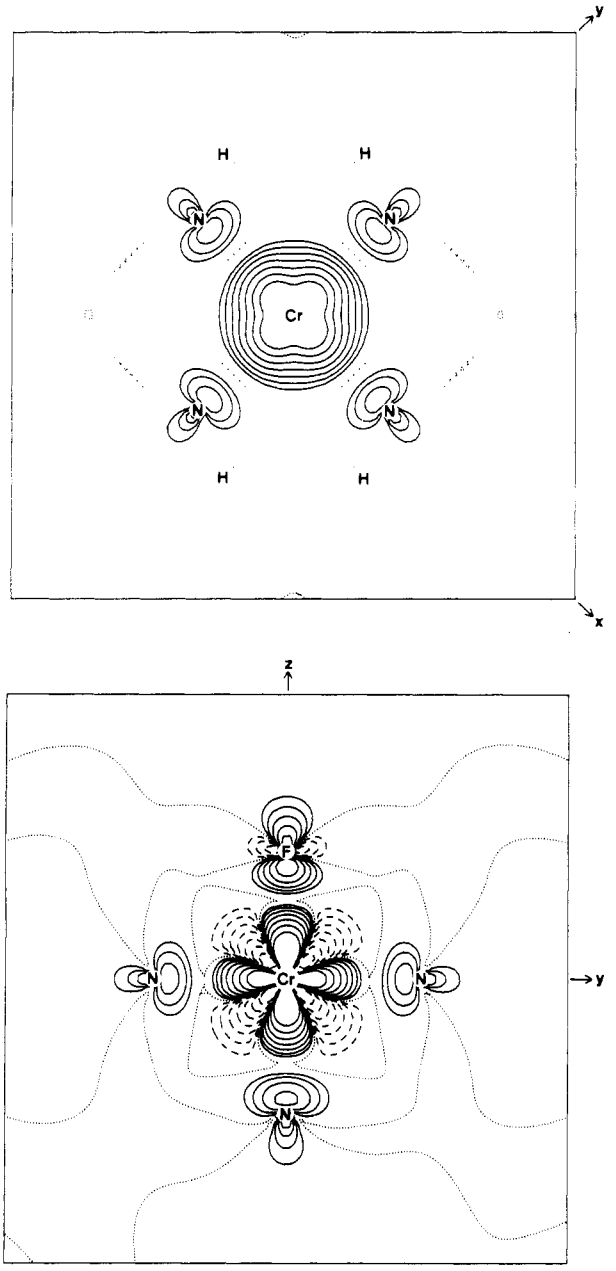

Figure 2. Total density difference plots $\rho(^4E) - \rho(^4B_1)$ for the $Cr(NH_3)_5F^{2+}$ complex. Part a (top) describes the density shifts in the xy plane upon excitation from the $^4B_1$ ground state to the photoactive state; part b (bottom) describes the density shifts in the yz plane. Full contours correspond to an increase in electron density and dashed contours to a decrease in electron density. At the dotted lines $\Delta\rho = 0$. The values of the $\Delta\rho$ contours are ±0.00125, ±0.0025, ±0.005, ±0.01, ±0.02, ±0.04, ±0.08, and 0.0 au^{-3}.

coordinated fragments have a less ephemeral existence in the solid than in solution, so that direct detection could become possible. In this respect it seems particularly interesting that the solid-state reaction has the same photostereochemistry as the solution reaction. Internal rearrangement of a pentacoordinated fragment is certainly possible in the solid.[65]

In previous publications[7,22] the angular overlap model was used in order to calculate the relative energies of the ligand field states for all four isomers. The results for the $Cr(NH_3)_4F^{2+}$ fragment are shown in Figure 3A. Figure 3 also displays the correlation of these states along the Berry interconversion paths. Correlations

(65) Note that the analysis in this section refers to complexes with monodentate ligands only. It is possible that chelating ligands may hinder some of the rearrangement paths considered and thus alter the photostereochemistry.

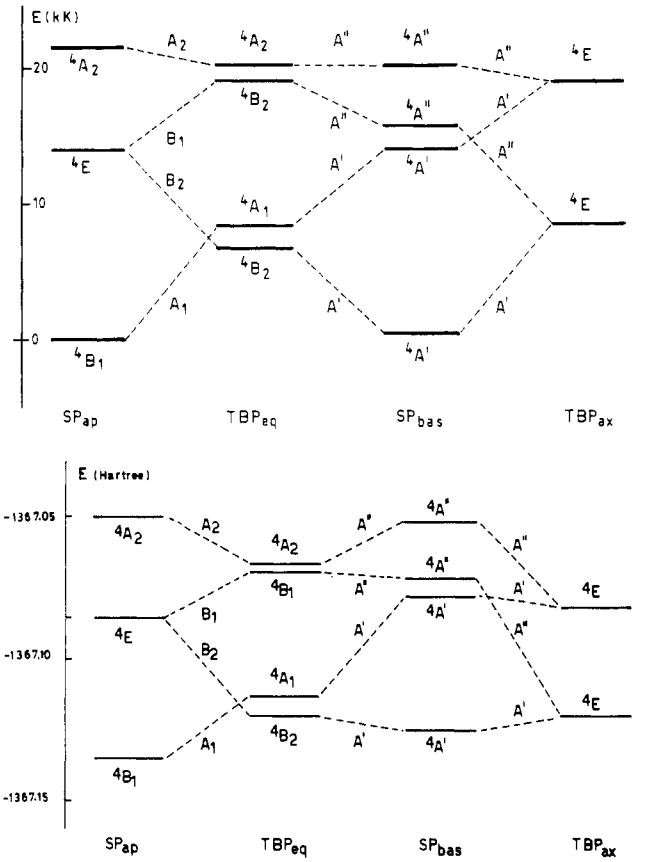

Figure 3. State correlation diagram for the isomerization of the $Cr(NH_3)_4F^{2+}$ fragment, calculated by ligand field (A, top) and ab initio methods (B, bottom). For each structure, the energies are the result of a CI calculation considering all states originating from the d^3 configuration. The CI calculation in B was performed within a frozen orbital approach, using the Av(d^3) orbitals.

for an alternative non-Berry rearrangement path were explored as well,[22] but this alternative reaction mode proved to be unfavorable. In order to test the validity of the ligand field approach, we have recalculated the SP and TBP structures of $Cr(NH_3)_4F^{2+}$ and $Cr(NH_3)_4Cl^{2+}$ with the ab initio method. In these calculations metal–ligand bond distances were not varied and bond angles were taken to be 90° in the SP structures, and 90 or 120° in the TBP structures. The results for $Cr(NH_3)_4F^{2+}$ are shown in Figure 3B.

The coincidence between the diagram obtained from the ligand field calculations and from the ab initio diagram is truly remarkable. A similarly gratifying correspondence is found for the $Cr(NH_3)_4Cl^{2+}$ fragment.[66] These observations corroborate the use of simple ligand field calculations to rationalize photochemical reactivity of transition-metal complexes.

b. d Orbitals of the $Cr(NH_3)_4X^{2+}$ Fragments. Before analyzing the state correlation diagrams in detail, it is interesting to take a closer look at the d orbitals of the $Cr(NH_3)_4X^{2+}$ fragments. Within ligand field theory, the d orbitals of the SP_{ap} and the TBP_{ax} intermediates (Figure 1) have the same composition as the orbitals of the hexacoordinated starting compounds, i.e. they are given by $d_{x^2-y^2}$, d_{z^2}, d_{xy}, d_{xz}, and d_{yz}. Yet, when this familiar d set is used to construct the energy matrices for the TBP_{eq} and the SP_{bas} structures, an interaction element between $d_{x^2-y^2}$ and d_{z^2} shows up. For TBP_{eq}—omitting the terms in π_N—the relevant interaction matrix is given by[22]

	z^2	$x^2 - y^2$
z^2	$\sigma_X + (17/32)\sigma_N$	$(-13\sqrt{3}/32)\sigma_N$
$x^2 - y^2$	$(-13\sqrt{3}/32)\sigma_N$	$(75/32)\sigma_N$

and after diagonalization one obtains[67]

(66) Postelmans, D. Ph.D. Thesis, University of Leuven, 1989.

$$d_- = (\sin p)d_{z^2} - (\cos p)d_{x^2-y^2}$$
$$d_+ = (\cos p)d_{z^2} + (\sin p)d_{x^2-y^2} \quad (1)$$

where p is defined by

$$\tan 2p = \frac{-26\sqrt{3}\sigma_N}{32\sigma_X - 58\sigma_N} \quad (2)$$

If X = N, the TBP skeleton has D_{3h} symmetry, $\tan 2p \rightarrow \sqrt{3}$, $p \rightarrow -60°$, and eq 1 becomes

$$d_- = (\sqrt{3}/2)d_{z^2} + (1/2)d_{x^2-y^2} = d_{z^2-y^2}$$
$$d_+ = (-1/2)d_{z^2} + (\sqrt{3}/2)d_{x^2-y^2} = d_{x^2} \quad (3)$$

Hence, for a perfect D_{3h} symmetry, the resulting orbitals correspond to $d_{z^2-y^2}$ and d_{x^2}. If X differs from N, small deviations from $d_{z^2-y^2}$ and d_{x^2} will be found. As indicated by eqs 1 and 2, the d_{z^2} character of the d_- orbital will be larger than 75% when $\sigma_X < \sigma_N$ and smaller than 75% when $\sigma_X > \sigma_N$. This can be seen explicitly in Table IV. In the TBP_{eq} of $Cr(NH_3)_4Cl^{2+}$ ($\sigma_{Cl} < \sigma_N$) the d_- orbital has a d_{z^2} contribution of 80%; in the TBP_{eq} of $Cr(NH_3)_4F^{2+}$ ($\sigma_F > \sigma_N$) the d_{z^2} content amounts to 74%. Table IV also shows the ab initio composition of the $\tilde{d}_-$ and $\tilde{d}_+$ orbitals, which are just the corresponding molecular orbitals of predominant d_- or d_+ character. As in ligand field theory, the Av(d^3) orbitals are approximately given by $\tilde{d}_{z^2-y^2}$ and $\tilde{d}_{x^2}$. Moreover, the ab inito results confirm that the $\tilde{d}_-$ orbital has a larger d_{z^2} contribution in the chloro- than in the fluoro-substituted TBP structure. Yet, also for the former, the ab initio method yields a smaller d_{z^2} contribution than in the perfect D_{3h} case. The reason for this discrepancy with ligand field theory is unclear.

In the C_{2v} symmetry of TBP_{eq} the $^4E'$ ground state of a d^3 trigonal bipyramid splits into two components of $^4A_1$ and $^4B_2$ symmetry. In the $^4B_2$ component the $\tilde{d}_-$ orbital (essentially $\tilde{d}_{z^2-y^2}$) is singly occupied, whereas in $^4A_1$, the $\tilde{d}_{yz}$ orbital is singly occupied. This different orbital composition can be visualized in a density difference plot for the $^4B_2 \rightarrow {}^4A_1$ transition (Figure 4). Figure 4 clearly shows that the densities of $^4B_2$ and $^4A_1$ are distributed over different regions in the TBP equator.

For the SP_{bas} structures, the AOM interaction matrix corresponds to

	z^2	x^2-y^2
z^2	$(7/4)\sigma_N + (1/4)\sigma_X$	$(\sqrt{3}/4)(\sigma_N - \sigma_X)$
x^2-y^2	$(\sqrt{3}/4)(\sigma_N - \sigma_X)$	$(9/4)\sigma_N + (3/4)\sigma_N$

and p in eq 1 is now defined as

$$\tan 2p = \frac{-\sqrt{3}(\sigma_N - \sigma_X)}{\sigma_N + \sigma_X} \quad (4)$$

Clearly, when X = N, the resulting eigenvectors are the pure d_{z^2} and $d_{x^2-y^2}$ orbitals. However, when X differs from N, these orbitals mix and this mixing becomes larger as the difference $\sigma_N - \sigma_X$ becomes greater. For the SP_{bas} structure of $Cr(NH_3)_4F^{2+}$, it appears that $\sigma_N - \sigma_X$ is so small that its effect is not noticeable (Table IV). When X corresponds to the Cl^- ligand, $\sigma_N - \sigma_X$ is almost four times larger but even in this case, the d_- orbital has a d_{z^2} content of 99%. The ab initio calculations clearly confirm these small deviations. As a matter of fact, for both SP_{bas} intermediates, no significant mixing of d_{z^2} and $d_{x^2-y^2}$ is found. Figure 5 shows the $\tilde{d}_{z^2}$ orbital, which is the LUMO of the SP ground state. Clearly this orbital is directed toward the vacant coordination site. It therefore will attract an incoming nucleophile to restore the original hexacoordinated structure.[68]

c. Woodward–Hoffmann Approach to Photostereochemistry. Ligand loss of a hexacoordinated fragment in its first excited quartet state produces a square-pyramidal fragment in an excited state. For the case of *axial* labilization the photoactive ^4E state of the starting complex (*trans*-$Cr(NH_3)_4Cl_2^+$, $Cr(NH_3)_5X^{2+}$) correlates with the ^4E state of the SP_{ap}. The $\tilde{d}_{z^2}$ orbital, which is singly occupied in this state, is an almost pure $\tilde{d}_{z^2}$ orbital. For the ^4E state of the $Cr(NH_3)_4F^{2+}$ and $Cr(NH_3)_4Cl^{2+}$ fragments our ab initio calculations point to a $\tilde{d}_{z^2}$ contribution of respectively 93% and 94%, to be compared with AOM results of respectively 92% and 94%. So in the SP_{ap} the ^4E components are approximately described by

$$\Psi(^4E_x) \approx |(xz)^+(xy)^+(z^2)^+|$$
$$\Psi(^4E_y) \approx -|(yz)^+(xy)^+(z^2)^+|$$

On the other hand *equatorial* NH_3 loss of $Cr(NH_3)_5F^{2+}$ gives rise to the SP_{bas} fragment. As this dissociation process lowers the symmetry to C_s, the photoactive ^4E state will split into $^4A' + {}^4A''$. Both ligand field theory (Figure 3A) and ab initio calculations (Figure 3B) predict that the lowest excited component will be $^4A'$. This component corresponds to a $\tilde{d}_{xz} \rightarrow \tilde{d}_{z^2}$ excitation, which is symmetric with respect to the xz symmetry plane containing the heteroligand and the leaving ligand. The actual $\tilde{d}_{z^2}$ content is 93% at the ab initio level and 94% according to ligand field theory.

Once these starting states have been defined, the course of the rearrangement reaction can be analyzed from the correlation diagrams, using the familiar Woodward–Hoffmann (WH) approach. It is clear that the ^4E state of SP_{ap} correlates via the $^4B_2$ state of TBP_{eq} with the ground state of the SP_{bas} fragment. As we have indicated before, this ground state will immediately coordinate a solvent molecule at its vacant coordination site, which is cis with respect to the heteroligand. Hence the following reaction sequence is expected:

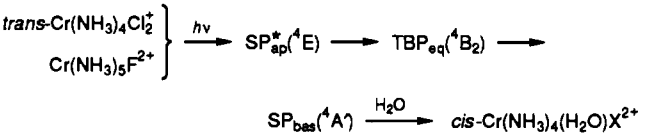

This sequence explains the observed trans → cis stereomobility of the photoreaction. For the case of equatorial ligand loss in $Cr(NH_3)_5F^{2+}$, a complication arises since the starting SP can rearrange to both TBP isomers. However it is clear from the diagrams in Figure 3 that the relevant excited $^4A'$ component of SP_{bas} correlates with a ground-state component of TBP_{eq} but with an excited state of TBP_{ax}. This implies that the $SP_{bas} \rightarrow TBP_{eq}$ rearrangement will be greatly favored over the $SP_{bas} \rightarrow TBP_{ax}$ rearrangement. This selective relaxation path obeys the following general rule.[7]

In the lowest excited quartet, the plane of excitation is formed by the two axes of weakest average ligand field. Upon removal of a ligand from this plane, the resulting T-shaped structure will rearrange to an equilateral triangle. The perpendicular axis is conserved. If there are two equivalent weak-field planes, the rule yields the same result when applied to either one of them.

Table IV. d_{z^2} and the $d_{x^2-y^2}$ Contributions to the d_- and d_+ Orbitals (Eq 1) of the TBP_{eq} and SP_{bas} Structure of $Cr(NH_3)_4F^{2+}$ and $Cr(NH_3)_4Cl^{2+}$ [a]

			d_-		d_+	
compound	structure	method	% d_{z^2}	% $d_{x^2-y^2}$	% d_{z^2}	% $d_{x^2-y^2}$
$Cr(NH_3)_4Cl^{2+}$	TBP_{eq}	AOM	80	20	20	80
		ab initio	72	28	27	74
	SP_{bas}	AOM	99	1	1	99
		ab initio	100	0	0	100
$Cr(NH_3)_4F^{2+}$	TBP_{eq}	AOM	74	27	27	74
		ab initio	68	32	32	68
	SP_{bas}	AOM	100	0	0	100
		ab initio	100	0	0	100

[a] At the ligand field level, these contributions result from a diagonalization of the relevant ligand field interaction matrices; the ab initio contributions are based on the Mulliken gross populations for the Av(d^3) orbitals.

(67) McGlynn, S. P.; Vanquickenborne, L. G.; Kinoshita, M.; Carroll, D. G. *Introduction to Applied Quantum Chemistry*; Holt Rinehart and Winston Inc.: New York, 1972.
(68) Rossi, A. R.; Hoffmann, R. *Inorg. Chem.* **1975**, *14*, 365.

In the present example the plane of excitation is the *xz* plane. Rearrangement of the ligands in this plane will uniquely lead to a TBP_{eq} structure, in agreement with the correlation diagram. Via this TBP_{eq} fragment the system finally raches the ground state of the opposite SP_{ap} fragment. Hence for equatorial ligand loss in $Cr(NH_3)_5F^{2+}$ the following reaction sequence is expected:

$$Cr(NH_3)_5F^{2+} \xrightarrow[-(NH_3)_{eq}]{h\nu} SP^{*}_{bas}(^4A) \longrightarrow TBP_{eq}(^4A) \longrightarrow$$

$$SP_{ap}(^4B_1) \longrightarrow trans\text{-}Cr(NH_3)_4(H_2O)F^{2+}$$

According to this scheme equatorial ligand loss of $Cr(NH_3)_5F^{2+}$ should produce 100% of the trans isomer. Although this isomer is indeed the dominant photoproduct, it is probable that some cis product is being formed as well (see Section II). Rationalization of this deviating behavior apparently requires a closer examination of the multidimensional potential energy surfaces involved. This can be accomplished by a Jahn–Teller type treatment.

d. Jahn–Teller Approach to Photostereochemistry. A detailed Jahn–Teller treatment (JT) of the pentacoordinated fragments has been presented elsewhere.[69] Here we will mainly be concerned with the connection between the JT and WH approaches. To a certain extent both approaches are complementary to each other: the WH analysis yields one-dimensional sections through the reaction surface, while the JT treatment indicates how these sections must be put together to form the backbone of a multidimensional surface.

If the five ligands were equal, the deactivation of the excited SP fragments could be situated on a two-dimensional JT surface, centered on a TBP fragment. In D_{3h} symmetry, such a fragment has a $^4E'$ ground state which is indeed strongly JT active under an e′ equatorial bending mode. The resulting degeneracy lifting leads to a double-sheeted E′ × e′ surface characterized by the familiar Mexican hat structure, with the TBP as the central pivot point and three equivalent SP fragments in three surrounding minima. As shown in Figure 6, each of the three equatorial ligands of the TBP can move to the apical position of a square pyramid. In the preceding section WH correlation diagrams were constructed for the three TBP ↔ SP interconversion paths. These paths are now recognized as specific routes on a two-dimensional E′ × e′ surface, that functions as a global deactivation channel. It is important to realize that the structure of this surface is not greatly altered by the introduction of heteroligands. The primary effect of substituents is to displace the crossing point between upper and lower sheet.[69] For the $Cr(NH_3)_4X^{2+}$ fragments the degeneracy point is found along the $SP_{ap} \leftrightarrow TBP_{eq}$ path, where the $^4A_1$ and $^4B_2$ states cross (see Figure 3). The corresponding JT surface may schematically be represented as follows:

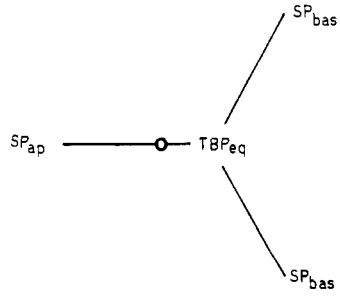

Here the circle indicates the position of the 2-fold degeneracy. Upon ligand loss a system will enter the upper surface at a square-pyramidal structure. Subsequent decay will populate the SP ground-state wells on the lower surface. These ground states will then be trapped by solvent molecules to yield the hexacoordinated photoproducts. Since this final process is very efficient and does not require activation energy, the SP ground states will probably not live long enough to allow thermal interconversion between the three SP minima on the lower surface. This leaves the decay process itself as the primary controlling factor of the product stereochemistry. In a one-dimensional WH picture it is automatically implied that the tunneling through the intersection region conserves the symmetry of the state and thus follows a straight-line trajectory. Hence one would expect selective population of the SP ground states that are at the opposite side of the crossing point. However in the perspective of a JT analysis deviations of such transverse tunneling path are possible, as the path may extend in two dimensions. This could result in a loss of selectivity during the tunneling through the conical intersection, and eventually lead to a random population of the three isomeric wells. In this respect, the following interesting correlation seems to hold and can tentatively be considered as a second general rule.

In all cases where the crossing point of the upper and lower surfaces is displaced *toward* the excited-state entrance point, the preference for selective transverse tunneling is most pronounced. In cases where the crossing point is displaced *away* from the entrance point, the directional selectivity is partly lost and a more random decay will be observed.

This rule effectively integrates the second and third stereochemical rules presented in our previous work.[7]

Hence in the case of axial ligand loss the entrance point is the excited state of SP_{ap}, which is close to the crossing point of upper and lower surface. This seems to favor selective transverse decay to the opposite SP_{bas} wells, giving rise to almost 100% cis product. On the other hand equatorial ligand loss prepares a $Cr(NH_3)_4F^{2+}$ fragment in the excited state of the SP_{bas} structure. This entrance point is further away from the crossing point. Accordingly population of the SP_{ap} well at the opposite side of the intersection will be less selective. This is reflected in the reduced stereomobility (70%) of the equatorial photoreaction in $Cr(NH_3)_5F^{2+}$.

e. Photostereochemistry of the Difluoro Complexes. As a further interesting application of the rules, presented in the preceding sections, we may now consider the photostereochemistry of the *cis*- and *trans*-difluoro complexes. In both isomers the original plane of excitation is seen to contain the two heteroligands. According to our first rule this implies that a NH_3–Cr–NH_3 axis, perpendicular to the plane of excitation, will not be affected by subsequent rearrangement reactions. Formation of the *fac* product is thus disallowed, in excellent agreement with the experimental results of Kirk and Frederick.[29]

Rearrangement of the ligands in the plane of excitation gives access to the upper sheet of a JT surface, centered at a TBP structure with both substituents in the equatorial plane, e.g. TBP_{ee}. The SP isomers on the JT wheel around this TBP may be denoted as SP_{trans} and SP_{cis}.

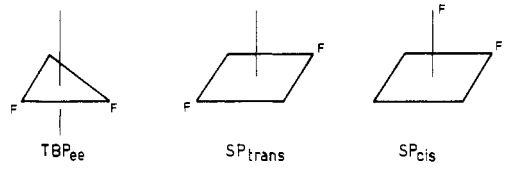

Since the equatorial triangle now contains two F ligands and one NH_3 ligand, the energy of the d_{yz} and $d_{z^2-y^2}$ orbitals is reversed with respect to the monofluorocomplex, and also the order of the $^4A_1$ and $^4B_2$ levels in Figure 3 is reversed. The JT surface can therefore schematically be represented as

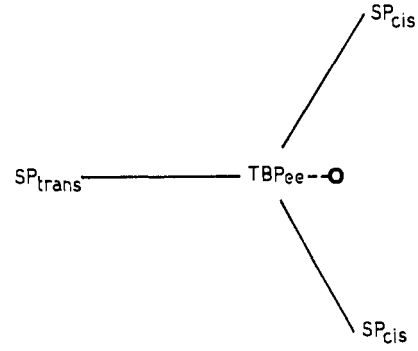

(69) Ceulemans, A. In *Vibronic Processes in Inorganic Chemistry*; Flint, C. D., Ed.; Kluwer: Dordrecht, The Netherlands, 1989; p 221.

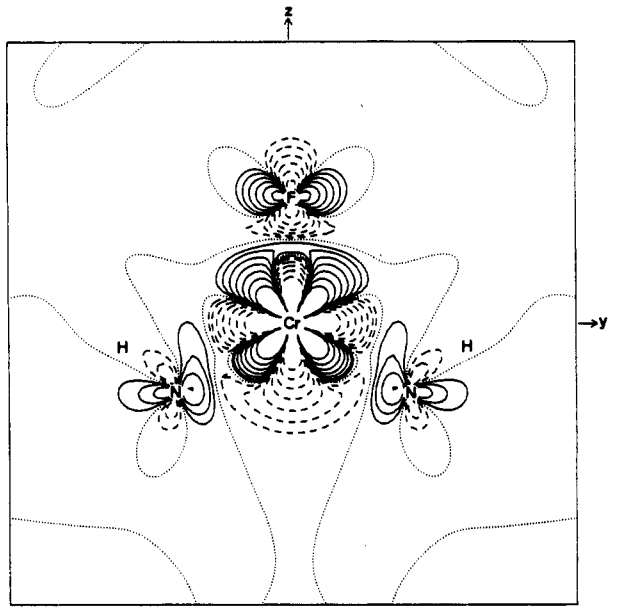

Figure 4. Total density different plot $\rho(^4A_1) - \rho(^4B_2)$ for the TBP_{eq} of the $Cr(NH_3)_4F^{2+}$ fragment. This figure describes the density shifts in the *yz* plane on going from the $^4B_2$ ground state to the $^4A_1$ level. On the orbital level this approach corresponds to a $d_{z^2-y^2} \rightarrow d_{yz}$ excitation. Full contours correspond to an increase in electron density and dashed contours to a decrease in electron density. At the dotted lines $\Delta\rho = 0$. The values of the $\Delta\rho$ contours are ±0.00125, ±0.0025, ±0.005, ±0.01, ±0.02, ±0.04, ±0.08, and 0.0 au^{-3}.

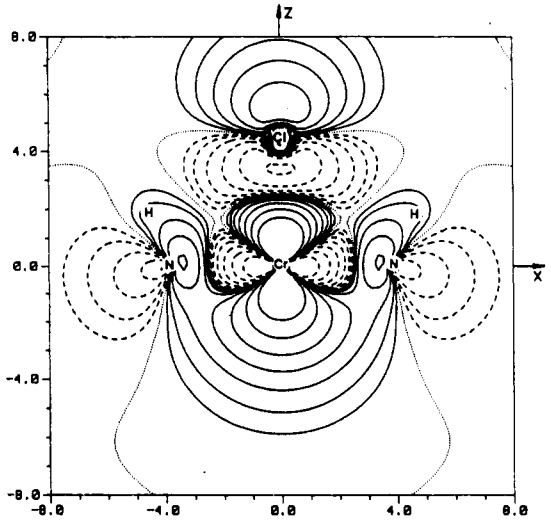

Figure 5. $\tilde{d}_{z^2}$ orbital in a square-pyramidal $Cr(NH_3)_4Cl^{2+}$ fragment, as obtained from an ab initio calculation of the ^4E ($d^1_{z^2}$, d^1_{xy}, $d^{0.5}_{yz}$) excited state. Contour values are 0.0, ±0.16, ±0.08, ±0.04, ±0.02, ±0.01, ±0.005, and ±0.00125 $au^{-3/2}$.

The circle indicates that the pivotal point lies on the straight line that contains the $SP_{trans} \leftrightarrow TBP_{ee}$ path, but beyond the TBP origin. This means that it will not show up in a straightforward WH analysis, which is confined to the SP ↔ TBP interconversion paths.

Photolysis of the trans complex prepares the $Cr(NH_3)_3F_2^+$ fragment in the excited state of the SP_{trans} isomer. Since this entry point is not close to the intersection point, one should expect a more random population of the three SP isomers. The actual product distribution (30% *mer*-FWF, 70% *mer*-FFW) is indeed quite close to the random distribution (33% *mer*-FWF, 66% *mer*-FFW). On the other hand photolysis of *cis*-$Cr(NH_3)_4F_2^+$ is predicted to be more selective. In this case a transverse crossing, starting from an excited SP_{cis} entry point, would populate both a trans and a cis SP isomer. This would lead to a 50:50 mixture of the two meridional products, which is indeed close to the observed product ratio (45% *mer*-FWF, 55% *mer*-FFW).

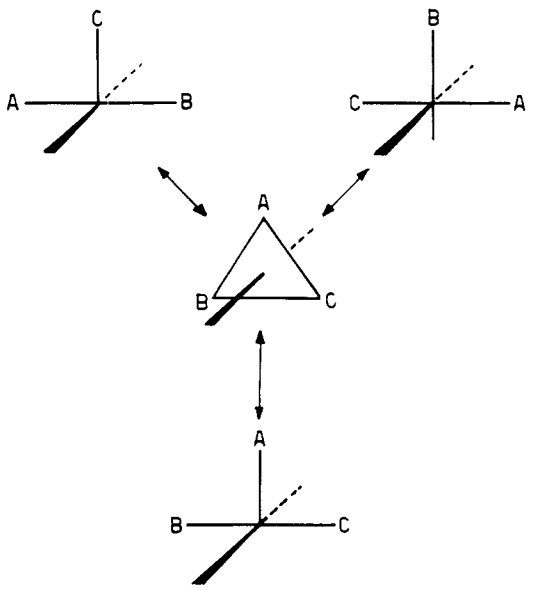

Figure 6. Schematic representation of the isomerization pathways of a trigonal-bipyramidal fragment. Each of the three equatorial ligands can move to the apical position of a square pyramid.

Therefore, the correlation between the position of the pivotal point and the selectivity of the decay process, which was noted for the photochemistry of the monofluoro compound, also seems to hold in the case of the difluoro complexes.

VI. Conclusions

Within a dissociative approach, it has been shown that ab initio calculations at the ligand field CI level are able to give a satisfactory rationalization of the observed photochemical behavior of the $Cr(NH_3)_5F^{2+}$ compound, *trans*-$Cr(NH_3)_4Cl_2^+$, and the cis and trans isomers of $Cr(NH_3)_4F_2^+$. It follows from the relative state energies that the photochemistry of the cis compound proceeds via $^4B_2$ population, while the photochemical substitution processes in the other complexes originate in the ^4E state. By analysis of the electron density shifts upon excitation to these photoactive states, the preferential leaving ligand was characterized. The dominant reaction modes were predicted to be axial NH_3 loss for the $Cr(NH_3)_5F^{2+}$ compound, Cl^- loss for the disubstituted chloro complex, and aquation of one of the $(NH_3)_{eq}$ ligands for the $Cr(NH_3)_4F_2^+$ isomers. These results are in perfect agreement with experiment.

The ab initio calculations have also been extended to the $Cr(NH_3)_4F^{2+}$ and $Cr(NH_3)_4Cl^{2+}$ fragments, with a square-pyramidal or trigonal-bipyramidal structure. Woodward–Hoffmann correlation diagrams between these structures were found to be in remarkable agreement with the previously obtained results from an AOM analysis.

Both the ab initio and the ligand field calculations sustain two important stereochemical rules. The first rule states that ligand rearrangements are confined to the original plane of excitation. The second rule claims a preference for stereomobile reactions, due to selective transverse decay through a reaction funnel. This second rule summarizes the second and third stereorules of our earlier[7] analysis. The combination of these two rules in one was made possible by combining the WH correlation diagrams for three SP ↔ TBP interconversions into a single surface, in the framework of a Jahn–Teller description.

Acknowledgment. We are indebted to the Belgian Government (Programmatie van het Wetenschapsbeleid) for financial support. A.C. and K.P. thank the Belgian National Science Foundation (NFWO) for a research grant.

Registry No. $Cr(NH_3)_5F^{2+}$, 19443-25-5; *trans*-$Cr(NH_3)_4F_2^+$, 58864-86-1; *trans*-$Cr(NH_3)_4Cl_2^+$, 22452-49-9; *cis*-$Cr(NH_3)_4F_2^+$, 31253-66-4; $Cr(NH_3)_4Cl^{2+}$, 138259-85-5; $Cr(NH_3)_4F^{2+}$, 138259-86-6.